ANALYSIS OF COMMUNICATION RATES IN THE PROXIMITY OF NEAR-EARTH ASTEROIDS

Evan Nelson, Charles D. Creusere, Thomas Critz, Eric Butcher*

Klipsch School of Electrical and Computer Engineering
Department of Mechanical and Aerospace Engineering
New Mexico State University, Las Cruces, NM

ABSTRACT

In this paper we analyze fundamental local-area communication issues related to proximity operations around near-earth asteroids. We are motivated by NASA's plan to send robotic spacecraft to numerous such asteroids in the coming years in preparation for an eventual manned mission. We consider here the case where multiple probes are deposited on the surface of an asteroid and must communicate the data they collect to each other and to earth by using the orbiting 'mothership' as a relay. With respect to this scenario, we statistically analyze the ability of surface probes in various locations to communicate with the mothership as well as their abilities to network with one another. For the purposes of this analysis, we assume the simplest possible communications scenario: a surface probe can communicate with the mothership only when it has an unobstructed line of sight. At the frequencies of interest here, line of sight is a necessary condition but it is obviously not sufficient—the end-to-end link margins of our communications system must be high enough to support the desired/required data rates. The work presented in this paper extends our previous research in which we only analyzed the the visibility of the locations on the surface of the asteroid. Here, we consider how visibility affects the required communications bandwidth and buffer sizes for both surface-to-spacecraft and surface-to-surface scenarios.

Keywords: Space communications, space communication networks, NEA missions, asteroid surface to space networking.

1 INTRODUCTION

Recently, there has been a great deal of interest in sending robotic precursor missions to near-earth asteroids (NEAs) for scientific study and to prepare for a possible manned mission in the mid-2020s. In particular, increased understanding of these small irregularly-shaped bodies is essential to the development of an NEA deflection strategy which might someday be implemented for planetary protection. In the far future, NEAs might also serve as fueling stations, mining sites, or remote observatories, and recent interest in asteroid exploration has been demonstrated by past, present, and future missions such as NEAR Shoemaker, Hayabusa, DAWN, and OSIRIS REx.

*Research supported by NASA/EPSCORE Grant 1065603

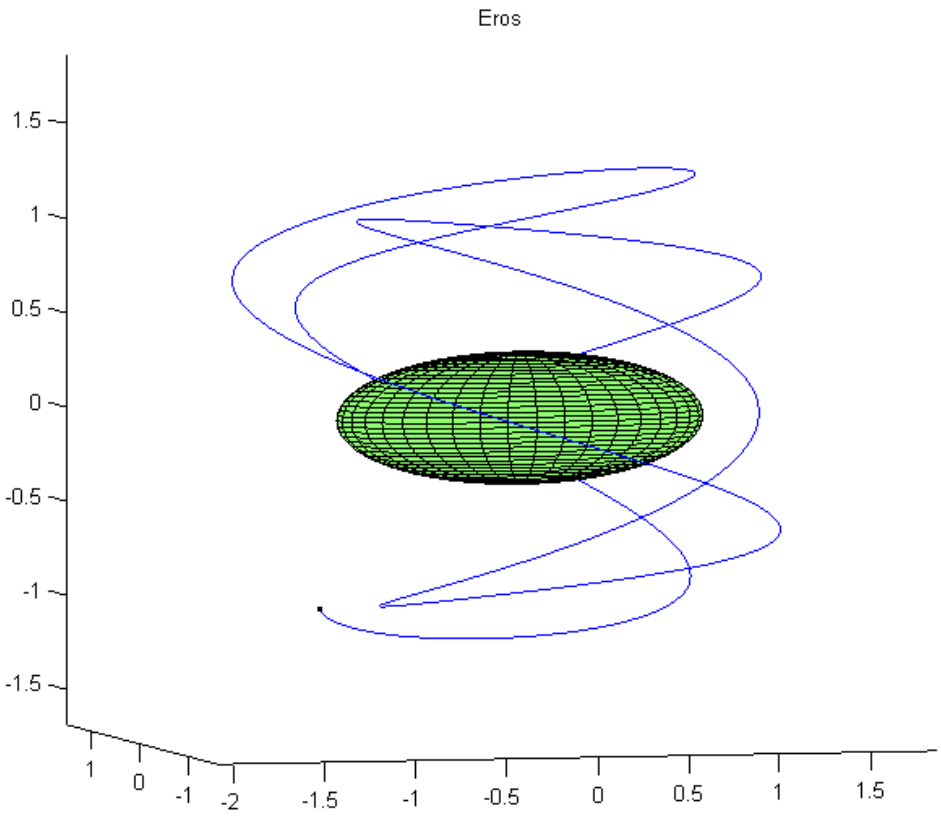

Figure 1: Simulated spacecraft orbit around asteroid Eros shown in the asteroid body-fixed frame.

The research presented here considers an issue that is likely to be critical to future NEA missions: communication and networking for supporting local operations in the vicinity of an asteroid. Our assumption here is that future missions to NEAs will deploy multiple sensing platforms once they arrive in the vicinity of the target asteroid—possibly additional autonomous spacecraft but certainly one or more surface platforms. While a great deal of research has been done in the area of space communications theory, low-cost transmitter/receiver designs, and even deep-space networking (e.g., [1, 2, 3, 4, 5, 6]), we have found no work that addresses the special challenges of establishing and maintaining local-area communications in the neighborhood of an NEA. The sensors on these various platforms must communicate their data to each other (in order to coordinate their actions) and ultimately back to earth, and this requires that an *ad hoc* local-area communication system be established. Furthermore, it seems likely that in most scenarios an orbiting spacecraft (i.e., the 'mothership') will be required to act as the relay for both surface-to-surface (between NEA-local sensor platforms) and surface-to-earth communication. This is the scenario we assume in the research presented here where a single orbiting spacecraft acts as the relay and six surface platforms communicate with each other and with earth through it.

Further narrowing our focus, we assume that if a surface platform has an unobstructed line-of-sight to the orbiting spacecraft, then it can communicate to and through that spacecraft. At the frequencies required for space operations due to antenna design constraints, line-of-sight is a necessary but not sufficient condition for establishing a communications link; thus, the results presented here can be viewed as the best-case scenario. An analysis of communication capacity or availability between surface platforms and a spacecraft orbiting a massive, roughly spherical body like the Earth is easily performed and therefore not of great interest. Many NEAs, however, are small, aspherical bodies having non-uniform mass distributions, and they not only allow for very irregular orbits but also often support a diversity of different orbits. Furthermore, the tumbling spin of many of these objects also causes significant variations in the communication connectivity for platforms at different locations on the surface. These factors combine to make the simulation results presented here non-trivial and of some importance as a first step in designing the local-area communication system for future missions to NEAs

This paper is organized as follows. Section 2 discusses the problem of orbital modeling. Section 3 discusses the simulation of data being buffered on the probes.

2 ORBITAL MODELING

In most orbital models, both the celestial body and its satellite are treated as point masses with the assumption being that the satellite's mass is insufficient to affect the motion of the celestial body. This assumption holds in most applications, since the gravitational field produced by a constant-density sphere mimics that of a point mass, and the discrepancies between a celestial body's true shape and mass distribution relative to a constant-density sphere can often be modeled as perturbation functions with respect to the ideal orbit model. This simplification does not hold for a typical asteroid, however. The irregular shape of an asteroid creates a gravitational field that is much more complex than that of a sphere, resulting in a scenario where the gravity experienced by a satellite depends not just on distance but also on its position relative to the asteroid. Moreover, since the asteroid is rotating, its gravitational field in inertial space changes with time.

We model the motion of a satellite about an asteroid in this work using the restricted full two-body approach described by Scheeres [7], in which the asteroid is depicted as a scalene ellipsoid with constant density in uniform rotation about its largest moment of inertia. By using this simplification, the asteroid can be fully described with five parameters (three semi-major axis lengths, density, and spin rate), all of which can be approximated from ground-based observations. Furthermore, changing these body parameters allows one to model a wide variety of asteroids.

In the restricted full two-body problem (RF2BP), a small body with negligible mass is considered to be under the influence of a large body's gravity. If the position of the satellite relative to a large, rotating body is described in a coordinate frame that is fixed to the gravitational body, the differential equation governing the motion of the satellite is

$$\ddot{\vec{r}} + 2\vec{\omega} \times \dot{\vec{r}} + \vec{\omega} \times (\vec{\omega} \times \vec{r}) + \dot{\vec{\omega}} \times \vec{r} = \frac{\partial U(\vec{r})}{\partial \vec{r}} \tag{1}$$

where $\overrightarrow{\Omega}$ describes the angular velocity of the asteroid, $\overrightarrow{r}$ is the position of the satellite, and $U(\overrightarrow{r})$ is the scalar force potential of the satellite caused by the asteroid's gravity. For the application of the RF2BP used in this paper, the origin of the coordinate frame used to describe $\overrightarrow{r}$ is placed at the asteroid's center of mass and its axes are aligned with the asteroid's principal moments of inertia. Furthermore, the asteroid is assumed to be rotating about its maximum moment of inertia with constant angular velocity ω. Equation (1) can be described in Cartesian form by the following equations[8]:

$$\ddot{x} - 2\omega\dot{y} - \omega^2 x = \frac{\partial U}{\partial x} \tag{2}$$

$$\ddot{y} + 2\omega\dot{x} - \omega^2 y = \frac{\partial U}{\partial y} \tag{3}$$

$$\ddot{z} = \frac{\partial U}{\partial z} \tag{4}$$

The scalar force potential $U(\overrightarrow{r})$ can be defined by any mathematical solution to Laplace's equation representing mass distribution across a real body[9]. The use of spherical harmonics is one such solution of the form

$$U(r,\theta,\phi) = \frac{\mu}{r}\sum_{l=0}^{\infty}\sum_{m=0}^{l}(\frac{r_0}{r})^l P_{lm}(\sin\phi)(C_l m\cos m\theta + S_{lm}\sin m\theta) \tag{5}$$

where $P_{lm}(q)$ is the associated Legendre polynomial in q, r is the scalar distance from the origin, and θ and ϕ are the latitude and longitude angles, respectively. Additionally, the coefficients of expansion C_{lm} and S_{lm} can be uniquely determined from the location of the center of mass and the inertia tensor described in the body-fixed frame. That is,

$$\begin{aligned}
c_{11}r_0 &= x_{cm}\\
s_{11}r_0 &= y_{cm}\\
c_{10}r_0 &= z_{cm}\\
-Mr_0^2c_{22} &= I_{zz} - I_{yy}\\
Mr_0^2(2c_{22} + C_{20} &= I_{yy} - I_{zz}\\
-Mr_0^2(-2c_{22} + C_{20} &= I_{zz} - I_{xx}\\
-Mr_0^2s_{22} &= I_{xy}\\
-Mr_0^2s_{21} &= I_{yz}\\
-Mr_0^2c_{21} &= I_{xz}
\end{aligned}$$

For a uniformly rotating triaxial ellipsoid of constant density, the definition of the body-fixed, body-centered (BCBF) coordinate frame used in (2)–(4) reduces a second-degree and order spherical harmonic expansion to one that only includes the c_{20} and c_{22} terms. The resulting form for $U(\overrightarrow{r})$ in Cartesian form is

$$U(x,y,z) = \mu(\frac{R_0}{r})(1 - \frac{c_{20}(x^2+y^2-2z^2}{2r^4} + \frac{3c_{22}(x^2-y^2)}{r^4})r = \sqrt{x^2+y^2+z^2} \tag{6}$$

where $\mu = GM$ is the gravitational parameter and r_0 is the reference radius length[8]. By substituting (6) into (2)–(4), a trajectory can be estimated over a any length of time from a given set of initial conditions $[x_0, y_0, z_0, \dot{x_0}, \dot{y_0}, \dot{z_0}]$.

Table 1: Parameters for orbital design model.

Orbital Model	a (km)	b (km)	c (km)	$2\pi/\omega$ (hr)	ρ (g/cm^3)	Initial Conditions $[x, y, z, \dot{x}, \dot{y}, \dot{z}]$
Vesta (1)	265	250	220	5.3	3.5	[0, 1.5, 0, 3, 0, 1, 1.35]
Vesta (2)	265	250	220	5.3	3.5	[0, 1.8, 1.2, 3.5, 0, -0.85]
Eros	20	7	7	5.27	3.2	[0, 1.5, 0, 1.95, 0, 0.65]
Gaspra	9.5	6	5.5	7	3.5	[0, 1.25, 0, 2.95, 0, 1.65]
Tempel2	8	4.25	4.25	8.9	1.0	[1.35, 0, 0, 0, -3, 0.35]
Ida	28	12	10.5	4.63	3.5	[0,1.45, 0, 2.15, 0, 0.4]

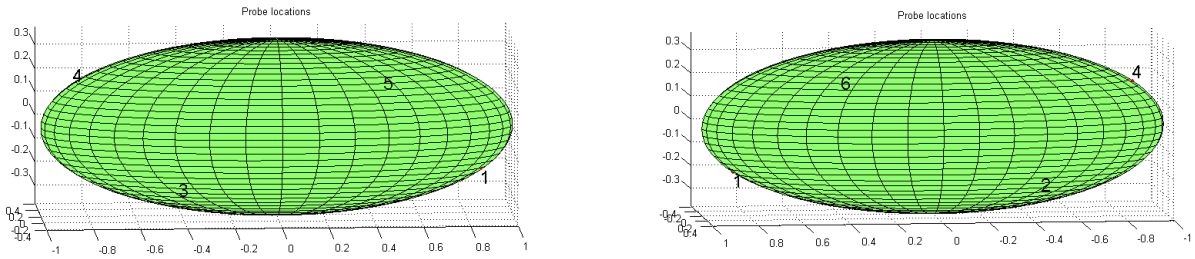

(a) (b)

Figure 2: Probe locations on the two sides of Ida.

We consider here the five orbital scenarios detailed in Table 1. Specifically, our test cases are as follows: Vesta (Orbits 1 & 2), Eros, Gaspra, Tempel2, and Ida. All of these asteroids have highly irregular shapes, but only one of them (Eros) is technically an NEA and Tempel2 is considered to be a comet. In every example considered here, we place six sensor on the surface of the asteroid in the following manner: three latitudes are chosen arbitrarily and the positions of the probes along each latitude line distributed as longitudinal pairs with reversed orientation in a semi-random fashion. What we mean by this is that if a single angle θ defines the longitudinal location of two sites at different latitudes, one site would be at $[\theta, \phi_1]$, then the other would be at $[\theta + \pi, \phi_2]$. Figure 2 illustrates the probe placement on asteroid Ida.

3 BUFFERING

For the scenario where the surface probes are generating data at a constant rate and the data needs to be transmitted to the orbiter, the probes must buffer this data until they have a chance to send it. By looking at the buffer fullness over time for a fixed (so that the amount of data in the buffer remains stable), we can get an idea of how big the buffer needs to be in the worst cast scenario. We can also infer from this analysis the minimum required communications rate between the probe and the orbiter, given the data generation rate of the probe.

In our simulations of the amount of data being buffered over time, the rate at which the data is generated by the surface probes was chosen to be 20 Kbits/s. The capacity of the communication channel between the orbiter and each surface probe was chosen to be at least 20 Kbits/s multiplied the inverse of the visibility probability of the specific surface probe—below this channel rate, the communication system will not be able to keep up with the data generation rate and the buffer will eventually overflow. Such an overflow would lead to lost sensor data. The minimum required channel capacity as given in (7) is increased by a factor α of either 0.1 or 0.2 in our simulations to ensure their stability. Table 2 shows the probability used to calculate the bit rates used in the simulations and Table 3 shows the bit rates used.

$$send\ rate = \left(\frac{1}{visiblilty\ probability} + \alpha \right) data\ rate \tag{7}$$

Table 2: Probablity of communication access.

Asteroid	probe 1	probe 2	probe 3	probe 4	probe 5	probe 6
Eros	0.27068	0.3394	0.3378	0.28576	0.34812	0.34672
Gaspra	0.23172	0.2968	0.29648	0.22172	0.28544	0.28696
Tempel2	0.47636	0.48868	0.48876	0.39432	0.43864	0.43776
Vesta #1	0.1396	0.14868	0.14772	0.15716	0.16556	0.16532
Vesta #2	0.23892	0.25204	0.2526	0.33864	0.3466	0.34644
Ida	0.1574	0.3322	0.3332	0.16508	0.33576	0.3354

Table 3: Communication rates for each probe $kbits/s$

Asteroid	probe 1	probe 2	probe 3	probe 4	probe 5	probe 6
Eros	76	62	62	74	60	60
Gaspra	90	70	70	94	72	74
Tempel2	44	44	44	54	48	48
Vesta #1	146	140	138	130	124	124
Vesta #2	90	84	84	62	62	62
Ida	132	62	62	124	62	62

The simulation of the size of the data in the buffers was done for 100 orbits and for the six different orbits. Figure 3-8 are plots of the amount of data in the buffers over time for

the different orbits. From looking at the plots of the simulations, for some orbits the amount of data in buffer tends to grow over certain periods of time. This is most prevalent in the orbit of Gaspra and Orbit #1 of Vesta. These show the data in buffer building up as orbit has less contact with those probes at those times as the orbits changes the data in buffers eventually starts to empty out. The plot for Vesta #1 in particular shows how the orbit favors probes 1-3 for part of the time and 4-6 for the remainder.

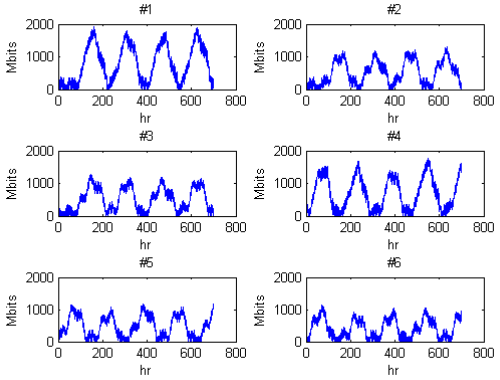

Figure 3: Buffer size over time for Gaspra

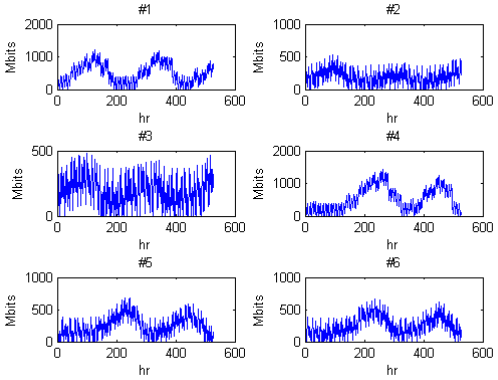

Figure 4: Buffer size over time for Eros

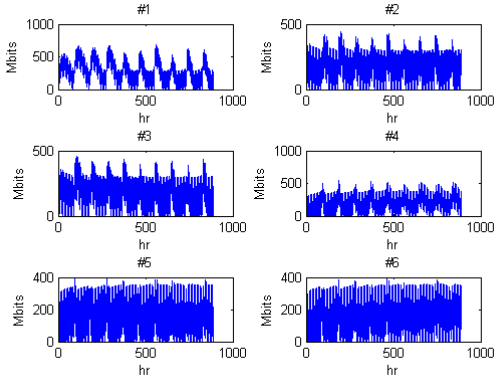

Figure 5: Buffer size over time for Tempel2

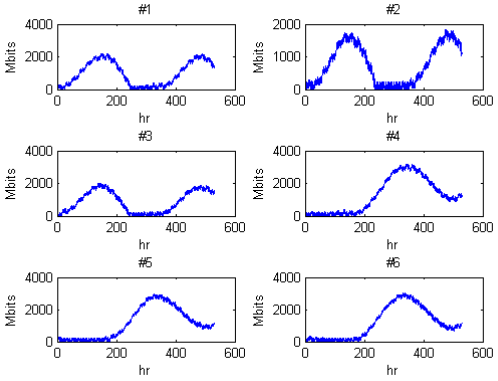

Figure 6: Buffer size over time for Vesta Orbit #1

4 Networking

In this section we look at the scenario where one probe on the surface of the asteroid has to communicate with another on the surface of the asteroid. In this case the orbiter must act as relay in order to facilitate communications. The simulation for this scenario measures the effective communication rate between each set of two probes. In the simulation the communications rate between the probes and the orbiter is chosen to be 100 Kbits/s. The effective networking rates between the probes listed in Tables 4 to 9 is average rate which data is transfered between the probes over 100 orbits around each of the asteroids.

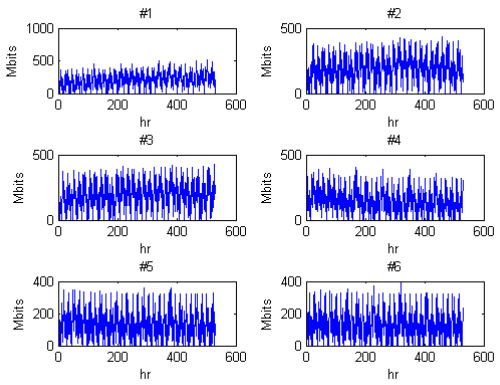

Figure 7: Buffer size over time for Vesta Orbit #2

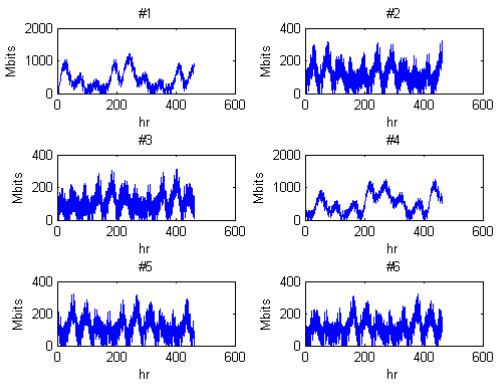

Figure 8: Buffer size over time for Ida

The effective data rate between to probe is limited by which of the two probes gets the least amount of communications contact with the orbiter as that would be the main bottleneck for either sending or receiving data. This allows for a good approximation for what the effective communications rate would be between to probes.

Rewrite the next sentence: it does not make sense! By multiplying the communication rate between the probes and the orbiter and multiplying it by the small of the two probabililties from Table 2 you get a good approximation of the effective rate.

Table 4: Gaspra effective networking rates between probes in kbits/s.

–	1	2	3	4	5	6
1		22.7083	22.5947	21.3168	22.0929	22.1948
2	22.7083		28.6236	21.6029	27.769	28.016
3	22.6064	28.7412		21.5441	27.82	27.8631
4	21.454	21.6813	21.5833		21.6304	21.6656
5	22.1909	27.7925	27.8239	21.6264		27.7337
6	22.2419	27.867	27.7847	21.65	27.6357	

Table 5: Eros effective networking rates between probes in kbits/s.

1	——	26.4247	26.3933	25.7504	26.3659	26.409
2	26.5227	——	32.8691	27.4713	32.6418	32.6731
3	26.456	32.8299	——	27.5379	32.7006	32.5202
4	26.3776	27.5301	27.4321	——	27.9064	27.8751
5	26.5266	33.1592	33.1043	28.0044	——	33.7472
6	26.5266	33.2611	33.0142	27.8751	33.7746	——

Table 6: Tempel2 effective networking rates between probes in kbits/s.

1	—	46.5811	46.6281	38.1375	42.4573	42.4024
2	46.6517	—	47.6473	38.4315	42.567	42.7395
3	46.6281	47.6395	—	38.4785	42.7866	42.5906
4	38.2551	38.4981	38.502	—	38.3766	38.3766
5	42.8297	42.8062	42.9865	38.5687	—	42.7042
6	42.7787	42.9002	42.7787	38.4903	42.7278	—

Table 7: Vesta orbit 1 effective networking rates between probes in kbits/s.

1	—	13.567	13.5121	13.3906	13.4416	13.4141
2	13.6062	—	14.2726	13.7787	14.2217	14.2373
3	13.5788	14.3824	—	13.7434	14.2569	14.1903
4	13.5435	13.8571	13.8257	—	15.2056	15.2056
5	13.6689	14.4608	14.4137	15.2761	—	16.0013
6	13.6807	14.4451	14.3549	15.2957	16.0444	—

5 Conclusion

In this paper, we have analyzed the communication rate for two different scenarios. First, we considered communications between the the orbiter and a surface probe; second, we looked at communications between two different probes on the surface using the orbiter as a relay. The analysis of the communications between the orbiter and the probe showed what the minimum communications rates could be and also how large the buffers would need to be in the worst case. In the analysis of communications between probes, we computed reasonable estimates of the communications rates for a variety of asteroids, probe placements, or orbits. Such simulations provide us with a useful tool for mission planning and system design so that data integrity can be ensured.

References

[1] E. Webb, "Ethernet for space flight applications," in *Aerospace Conference Proceedings, 2002. IEEE*, vol. 4, 2002, pp. 4–1927 – 4–1934 vol.4.

Table 8: Vesta orbit 2 effective networking rates between probes in kbits/s.

1	—	23.1553	23.1631	23.1004	23.3356	23.171
2	23.2337	—	24.4097	24.5429	24.6253	24.5351
3	23.2102	24.5939	—	24.5508	24.6841	24.4998
4	23.0063	24.4724	24.4606	—	33.159	33.1316
5	23.2337	24.5743	24.6331	33.163	—	33.6686
6	23.265	24.6057	24.4959	33.0806	33.8019	—

Table 9: Ida effective networking rates between probes in kbits/s.

1	—	15.4251	15.4094	15.3428	15.4094	15.4251
2	15.4251	—	32.3593	16.0993	32.3593	32.4809
3	15.4251	32.3633	—	16.0954	32.5593	32.3397
4	15.4251	16.1777	16.1267	—	16.0875	16.1777
5	15.4251	32.3868	32.6377	16.1777	—	32.5906
6	15.4251	32.5553	32.4848	16.1777	32.7278	—

[2] X. Hong, M. Gerla, H. Wang, and L. Clare, "Load balanced, energy-aware communications for mars sensor networks," in *Aerospace Conference Proceedings, 2002. IEEE*, vol. 3, 2002, pp. 3–1109 – 3–1115 vol.3.

[3] S. Burleigh, A. Hooke, L. Torgerson, K. Fall, V. Cerf, B. Durst, K. Scott, and H. Weiss, "Delay-tolerant networking: an approach to interplanetary internet," *Communications Magazine, IEEE*, vol. 41, no. 6, pp. 128 – 136, june 2003.

[4] J. Jackson, "The interplanetary internet [networked space communications]," *Spectrum, IEEE*, vol. 42, no. 8, pp. 30 – 35, aug. 2005.

[5] S. Farrell, V. Cahill, D. Geraghty, I. Humphreys, and P. McDonald, "When tcp breaks: Delay- and disruption- tolerant networking," *Internet Computing, IEEE*, vol. 10, no. 4, pp. 72 –78, july-aug. 2006.

[6] C. Cottingham, W. Deininger, R. Dissly, K. Epstein, D. Waller, and D. Scheeres, "Asteroid surface probes: A low-cost approach for the in situ exploration of small solar system objects," in *Aerospace conference, 2009 IEEE*, march 2009, pp. 1 –11.

[7] D. Scheeres, "Dynamics about uniformly rotating triaxial ellipsoids: application to asteroids," *Icarus*, vol. 110, no. 2, pp. 225 –238, august 1994.

[8] W.-D. Hu and D. Scheeres, "Periodic orbits in rotating second degree and order gravity fields," *Chinese Journal of Astronomy and Astrophysics*, vol. 8, no. 1, pp. 108–118, 2008.

[9] D. Scheeres, *Orbital Motion in Strongly Perturbed Environments, Applications to Asteroid, Comet and Planetary Satellite Orbiters*, 1st ed. Springer, 2012.